313 Ganglion Cells and Beyond
Tuesday, May 09, 2017 8:30 AM–10:15 AM
Exhibit/Poster Hall Poster Session
Program #/Board # Range: 2578–2600/A0168–A0190
Organizing Section: Visual Neuroscience

Program Number: 2578 **Poster Board Number:** A0168
Presentation Time: 8:30 AM–10:15 AM
Characterization of the nonlinear receptive fields of G9 and Off- alpha Ganglion cells in the rabbit retina
Iris Fahrenfort, Lian-Ming Tian, Stephen C. Massey, Stephen L. Mills. Ophthalmology and Visual Sciences, UTHealth, Houston, TX.
Purpose: The characterization of mammalian ganglion cells (GCs) has historically focused on the features of the classical receptive field, organized into the well-known center/surround. Recently, more attention has been given to the non-linear aspects of the receptive fields of GCs, which are involved in interesting features such as sensitivity to fine spatial detail of the stimulus. Several mechanisms have been implicated in changing the linear/non-linear ratio of different kind of GCs. Here, we aim to elucidate which mechanisms are responsible for the differences in spatial integration of G9GCs and OFF-alpha GCs.
Methods: Both classical and extra-classical receptive fields of G9 and Off-alpha GCs were probed with stimuli of different size, contrast, and spatial detail. The effect of L-AP4, SR95531, TPMPA, and strychnine on the linear to non-linear ratio were measured using both loose patch- and whole-cell voltage clamp- recordings.
Results: Despite the fact that both G9 GCs and Off-alpha GCs receive cross-over inhibition, the G9 GCs respond to contrast-reversing gratings in a linear manner whereas the Off-alpha GCs show highly non-linear behavior. L-AP4, SYM2081, SR95531, TPMPA and strychnine all modulate the linearity of both cell-types to some degree, independent of the initial linear/non-linear ratio.
Conclusions: Modulators of the ON-pathway, the OFF pathway and GABA-ergic transmission are all able to significantly change the linearity of their responses to contrast-reversing bars. The common effect of these drugs, i.e. the polarization of either the bipolar cells, the GCs, or both are likely to play a crucial role in how signals are processed and coded, and are unlikely to be fully explained by cross-over inhibition.
Commercial Relationships: Iris Fahrenfort, None; **Lian-Ming Tian**, None; **Stephen C. Massey**; **Stephen L. Mills**
Support: EY-10121, EY06515, Research to Prevent Blindness

Program Number: 2579 **Poster Board Number:** A0169
Presentation Time: 8:30 AM–10:15 AM
Simplified detection of ON/OFF receptive fields using a nonlinear input model
Hope Shi, Alexandra Boukhvalova, Daniel Butts, Joshua H. Singer. Biology, University of Maryland, College Park, MD.
Purpose: Retinal ganglion cells (GCs) often are classified as ON, OFF, or ON/OFF based on their responses to simple stimuli, like full-field, square wave flashes. Such analysis, however, fails to capture the computations performed within the receptive fields (RFs) of the GCs because the stimuli are spatially and temporally uniform. This problem often is addressed by the use of white noise stimuli, which permit the RFs of GCs to be mapped and the responses of the GCs to be described with linear-nonlinear (LN) models. LN analysis fails to describe the most numerous GCs in the rodent retina- ON/OFF cells, because it treats the circuitry presynaptic to the GC as a single input. Here, we use a spatially correlated noise stimulus combined with analysis by a novel, nonlinear input model (NIM) to: 1) demonstrate a methodology for characterizing ON/OFF GCs and 2) extract multiple parallel inputs to GCs. This approach is compared to LN analyses and demonstrated to offer several advantages.
Methods: Light responses of GCs in the ventral mouse retina were recorded using a 60-channel multi-electrode array mounted on an inverted microscope. UV light stimuli from a modified DLP projector were delivered through the objective. Stimuli included full-field square-waves, standard Gaussian white noise checkerboards, and spatially correlated ("cloud") noise generated by low-pass filtering the Gaussian checkerboards. RFs of GCs were characterized by a separable NIM, which describes the responses of GCs as reflecting the integrated outputs of excitatory and suppressive input subunits; the performance of the NIM was compared to that of a standard LN model. All parameters were determined using maximum a posterior optimization.
Results: LN analysis yielded descriptions of ON and OFF RFs (not those of ON/OFF RFs). NIM analysis, however, revealed a significant number of ON/OFF GCs. And, we observed a number of instances in which GCs that appeared to be either ON or OFF cells from their responses to square waves were found to be true ON/OFF cells by NIM. The ON/OFF nature of GCs revealed by NIM analysis was verified experimentally by observations of responses to repeated stimuli.
Conclusions: NIM analysis of responses to a cloud stimulus captures the real identity of GCs, describing their spike output as arising from the integration of excitatory and suppressive inputs. Thus, it provides a novel and useful framework for the study of retinal circuits.
Commercial Relationships: Hope Shi, None; **Alexandra Boukhvalova**, None; **Daniel Butts**, None; **Joshua H. Singer**, None
Support: University of Maryland, Department of Biology, Brain and Behavior Initiative seed grant

Program Number: 2580 **Poster Board Number:** A0170
Presentation Time: 8:30 AM–10:15 AM
Synaptic inputs to a gamma ganglion cell in rabbit retina
David W. Marshak[1], Andrea S. Bordt[1], Diego Perez[1], Luke Tseng[1], Weiley S. Liu[1], Crystal Sigulinsky[2], Daniel Emrich[2], James S. Lauritzen[2], Carl B. Watt[2], Bryan W. Jones[2], Robert E. Marc[2]. [1]Neurobiology & Anatomy, McGovern Medical School, Houston, TX; [2]John A. Moran Eye Center, Salt Lake City, UT.
Purpose: There are at least 30 distinct types of mammalian retinal ganglion cells, each sensitive to different features of the visual environment, and these can be grouped according to their morphology. One such group, the gamma cells, was identified more than 40 years ago, but their synaptic inputs have never been described. That was the goal of this study.
Methods: The synaptic inputs to a subtype of gamma cell with dendrites ramifying in the outer sublamina of the inner plexiform layer (IPL) of the rabbit retina were identified in a retinal connectome developed using automated transmission electron microscopy.
Results: The gamma cell was always postsynaptic in the IPL, confirming its identity as a ganglion cell. The local synaptic input should produce relatively weak OFF reposnses to stimuli confined to the center of the gamma cell's receptive field. It typically received only one synapse per bipolar cell from at least 4 types of OFF bipolar cells. Because bipolar cells vary in their response kinetics and contrast sensitivity. each type would provide a small, asynchronous excitatory input. The amacrine cells at the dyad synapses provided only a small amount presynaptic inhibition; reciprocal synapses were observed in only 3 of the 18 ribbon synapses. There was no glycinergic crossover inhibition, another local interaction that would enhance light responses. Local postsynaptic inhibition was somewhat

more common; in 6 instances, the bipolar cells presynaptic to the gamma cell or their electrically coupled neighbors also provided input to an amacrine cell that inhibited the gamma cell. The other amacrine cell inputs to the gamma cell should have a much greater impact on the light responses because they are far more numerous. These are from axons and long dendrites of GABAergic amacrine cells, and they provide 60% of all the input. This finding suggests that many types of stimuli in the receptive field surround or outside of the classical receptive field would provide potent inhibition to the gamma cell.

Conclusions: The synaptic inputs rsuggest that gamma cells in rabbit retina would have light responses like their homologs in mouse retina, OFF responses to small stimuli in the receptive field center that are suppressed by a variety of larger stimuli. Thus, they would signal object motion selectively.

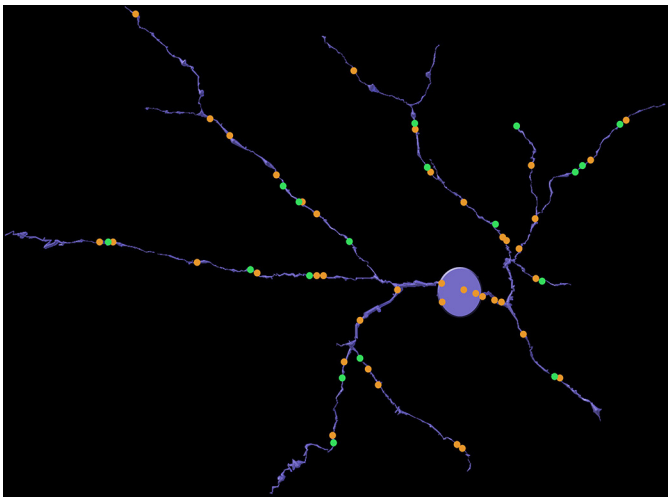

Synaptic inputs from bipolar cells (green) and amacrine cells (orange) to the gamma cell (purple).

Commercial Relationships: David W. Marshak, None; **Andrea S. Bordt**, None; **Diego Perez**, None; **Luke Tseng**, None; **Weiley S. Liu**, None; **Crystal Sigulinsky**, None; **Daniel Emrich**, None; **James S. Lauritzen**, None; **Carl B. Watt**, None; **Bryan W. Jones**, None; **Robert E. Marc**, Signature Immunologics (E)

Support: University of Texas BRAIN seed grant program 363303 (DWM PI), National Eye Institute Research Grant EY02576 (REM PI).

Program Number: 2581 **Poster Board Number:** A0171
Presentation Time: 8:30 AM–10:15 AM

Distinct Glycine Receptor Subunit Composition Across Retinal Ganglion Cell Types

Ian S. Pyle[1], Chi Zhang[3], Maureen A. McCall[2, 1]. [1]Anatomical Sciences and Neurobiology, University of Louisville, Louisville, KY; [2]Department of Ophthalmology and Visual Sciences, University of Lousiville School of Medicine, Louisville, KY; [3]Department of Biological Structure, University of Washington, Seattle, WA.

Purpose: Glycine inhibition shapes retinal signaling. Glycine receptors (GlyRs) are composed of the same β subunit and one of four α subunits. GlyRα subunits (GlyRαs) are differentially expressed in the inner retina and produce spontaneous inhibitory postsynaptic currents (sIPSCs) with distinct decay kinetics. These factors lead us to hypothesize that feedforward inhibition via specific GlyRαs will differentially modulate ganglion cell (GC) output. As a crucial step to addressing our hypothesis, we characterized expression of GlyRαs across 7 identified GCs.

Methods: Using mouse reporter lines (PV^{Cre}, TRHR, and W3), we recorded sIPSCs from fluorescently labeled GCs. Glycinergic sIPSCs were isolated in the presence of picrotoxin (PTX; 20μM) and confirmed in both PTX and strychnine (10μM). sIPSC frequency (over 100s) and τdecay of individual glycinergic sIPSCs were measured in WT GCs and used to devise hypotheses about GlyRαs expression. We compared sIPSC frequency (ANOVA) and τdecay (K-S test) in WT GCs with GCs from *Glra*2, 3 or 4 knockout (KO) mice or after *Glra*1 knockdown (KD) by injection of a retrogradely transported AAV-Glra1 shRNA construct into the LGN.

Results: Glycinergic sIPSC frequency and τdecay are similar across WT OFFα and ONα, ON_T and OFFδ GCs (X=26.5/s; 2.9ms, respectively), consistent with GlyRα1 expression. *Glra*1 KD eliminates glycinergic sIPSCs in these GCs. WT ON/OFF DS (ooDS) GC glycinergic sIPSC frequency is 5.7/s and τdecay is 21.6ms, consistent with expression GlyRα2 or α4. Although glycinergic sIPSCs frequency is unaltered in Glra2KO or Glra4KO ooDS GCs compared to WT, sIPSCs are eliminated in Glra2KO/Glra4KO ooDS GCs. WT mini-JAMB GC glycinergic sIPSC frequency is 14.1/s and τdecay is 6.5ms, consistent with GlyRα3 expression. sIPSC frequency drops significantly in both Glra2KO and Glra3KO GCs and sIPSCs are eliminated in Glra2KO/Glra3KO mini-JAMB GCs. WT local edge detector (LED) GC glycinergic sIPSC frequency is 14.3/s and τdecay is 7.5ms, consistent with GlyRα3 expression. sIPSC frequency drops significantly in both Glra3KO and Glra1KD GCs.

Conclusions: The 4 mouse GCs with the largest somas express only GlyRα1. Surprisingly, other GCs express GlyRαs with 2 distinct α subunit composition: ooDS GCs express GlyRα2 and α4, mini-JAMB's express GlyRα2 and α3 and LEDs express GlyRα1 and α3. These results serve as the basis for defining the role of specific GlyRαs in feedforward inhibition to GCs.

Commercial Relationships: Ian S. Pyle, None; **Chi Zhang**, None; **Maureen A. McCall**, None

Support: Sigma Xi: G201503151141261, RPB unrestricted grant to DOVS; NIH R01 EY014701

Program Number: 2582 **Poster Board Number:** A0172
Presentation Time: 8:30 AM–10:15 AM

Dependence of Flupirtine-resistant RGC oscillation in deafferentated mouse retinas on Connexin 36

Ching-Kang J. Chen[1, 2], Yu-Jiun Chen[1], Yu-Hsu Chen[1], Chih-Chun Hsu[2], Hung-Ya Tu[1]. [1]Ophthalmology, Baylor College of Medicine, Houston, TX; [2]Neuroscience, Baylor College of Medicine, Houston, TX.

Purpose: We showed recently by recording from cholinergic amacrine cells that in addition to the AII-amacrine cells (AII-AC) and ON-cone bipolar cells (ONCB) gap junction network, a Flupirtine-resistant oscillation mechanism exists in deafferentated mouse retinas (Front. Cell Neurosci. 9:513). The purposes of the study are to determine 1) the extent at which this novel mechanism drives retinal ganglion cell (RGC) oscillation and 2) whether the two prominent retinal connexins, Cx36 and Cx45, play any role.

Methods: Paired patch-clamp recordings were used to randomly survey 250 RGCs in the Nob mouse background for oscillating membrane potentials and their sensitivity to 15 uM Flupirtine. We used Fast Fourier Transform (FFT) to investigate if and whether a dominant oscillation frequency exists and to calculate the inhibition index (II) whereby sensitivity of oscillation to Flupirtine is defined. Some Nob mice were bred into the Cx36 knockout or the Cx45 conditional knockout background and the degree at which RGC

oscillation occurred therein was examined. We used biocytin and Lucifer Yellow in the internal solution to allow recovery of RGC dendritic morphology through *post hoc* immunohistochemistry and confocal microscopy. Voltage-dependent RGC intrinsic membrane properties were collected to facilitate cell type classification.
Results: The majority of recorded RGCs showed robust membrane potential oscillation but ~14% lacked such heitghtened activity. More than half of oscillating RGCs (~54%) ceased oscillation in the presence of Flupirtine, while ~9 % were completely resistant. Flupirtine treatment dampened oscillation of the rest ~23% of oscillating RGCs and to varying degrees. Consistent with the reported inhibition of Flupirtine-resistant OFF-SAC oscillation by the gap junction blocker meclofenamic acid (MFA), we found both ON- and OFF-SAC oscillation in Nob retinas to be absent when Cx36 but not Cx45 is genetically removed. A further random survey of 200 RGCs in the Nob/Cx36$^{-/-}$ double mutant mice found no oscillating RGCs.
Conclusions: These results demonstrated for the first time that the novel Flupirtine-resistant mechanism can exclusively drive certain RGC types to oscillate aindependent of the prominent AII-AC/ONCB mechanism and that Cx36 is needed for this novel mechanism. Cx45, another abundant retinal connexin, appears to have little/no role in RGC and SAC oscillation in the Nob mice.
Commercial Relationships: Ching-Kang J. Chen, None; **Yu-Jiun Chen**, None; **Yu-Hsu Chen**, None; **Chih-Chun Hsu**, None; **Hung-Ya Tu**, None
Support: NIH Grants EY013811, EY022228, EY002520, unrestrcted grant from Research to Prevent Blindness, Retina Research Foundation

Program Number: 2583 **Poster Board Number:** A0173
Presentation Time: 8:30 AM–10:15 AM
Retinal processing around saccades
Saad Idrees[1, 2], Thomas A. Muench[1, 3]. [1]Werner Reichardt Centre for Integrative Neuroscience, University of Tuebingen, Tuebingen, Germany; [2]IMPRS for Cognitive and Systems Neuroscience, Tuebingen, Germany; [3]Institute for Ophthalmic Research, Tuebingen, Germany.
Purpose: During natural viewing, image flow on the retina is determined primarily by the behavior of the observer. Eye movements during active visual exploration, such as saccades, are particularly dominating in this regard, especially because they incessantly occur 3-5 times per second. Despite this, retinal image processing has in the past often been studied with isolated stimuli, ignoring the highly dynamic aspects of natural viewing. We are therefore exploring the effects of eye-movement induced image motion on signal processing in the retina. We hypothesize that response of ganglion cells, to a stimulus following a saccade, is modulated as a function of time between the saccade and that stimulus.
Methods: We recorded activity of ganglion cells from isolated mouse and pig retina using multi-electrode arrays (MEA) while showing a visual stimulus paradigm mimicking saccades. The paradigm consisted of rapid saccade-like image shifts across the retina followed by a test stimulus at different intervals after the saccade.
Results: We found that the retinal responses to these "test stimuli", when presented in the context of saccades, are strongly modulated in comparison to responses to the same stimuli presented in isolation. Saccades exude their modulatory effects for up to 1 second, suggesting a highly relevant role of eye-movement induced effects under natural conditions with short inter-saccadic fixations. Such saccade-related retinal modulation critically depends on (1) the delay between saccade and test stimulus; (2) the statistical properties of the background scene present during the saccade; (3) the ambient luminance level; (4) and the specific retinal cell type. For example, the responses of OFF ganglion cells, but not ON ganglion cells, can be positively modulated after saccades.
Conclusions: Our results confirm our hypothesis that the response of ganglion cells to a stimulus following a saccade gets modulated. The results also indicate that the different pathways within the retina are distinct with respect to the properties of saccade-associated modulation. Thus, the diversity of modulations known from higher visual areas might, at least in part, be caused by the diverse modulations seen in the retina.
Commercial Relationships: Saad Idrees, None; **Thomas A. Muench**, None

Program Number: 2584 **Poster Board Number:** A0174
Presentation Time: 8:30 AM–10:15 AM
Effects of blocking GABA-C and mGlu1 receptors on contrast response functions of retinal ganglion cells in P23H rat
Ralph J. Jensen. Research, Boston VA Med Ctr, Boston, MA.
Purpose: Previous studies have shown that blocking GABA-C and mGlu1 receptors increase sensitivity of retinal ganglion cells (RGCs) in the P23H rat (a model of retinitis pigmentosa) to flashes of light. Here I examined the effects of blockers of these receptors on the contrast response functions of RGCs in P23H rat retina.
Methods: Following euthanasia of a rat with sodium pentobarbital, an eye was removed and hemisected. A square piece of retina was cut out and transferred with the ganglion cell side down onto a 64-channel planar Muse MEA (Axion Biosystems). A gravity-flow system provided carboxygenated Ames' Medium to the retina. The visual stimulus was a drifting sinusoidal grating (spatial frequency: 1 cycle/mm; temporal frequency: 2 cycles/s) that varied in stimulus contrast. The mean stimulus illuminance was held constant at 15 lux. Sorted spikes from RGCs were imported into Neuroexplorer software to create post-stimulus time histograms, averaged across 7 repetitions of the same contrast. Each histogram was Fourier transformed with OriginPro10 software to obtain the amplitude of the fundamental stimulus frequency (F1). Data were obtained before and during bath application of either the GABA-C receptor antagonist TPMPA (100 μM) or the mGlu1 receptor antagonist JNJ16259685 (0.5 μM).
Results: I have examined the effects of TPMPA and JNJ16259685 on the contrast response functions of over 80 P23H rat RGCs. I found that the effects of both TPMPA and JNJ16259685 were similar, in that these antagonists increased the responses of RGCs at all stimulus contrast levels. This is illustrated in the figure for one RGC that was treated with TPMPA. The data points fitted with the solid line are control values; the data points fitted with the dash line are values obtained in presence of TPMPA. For this cell, and many other cells, TPMPA and JNJ16259685 caused the curve to shift mainly vertically (i.e. an increase in response gain) rather than horizontally (i.e. an increase in contrast gain). Taking the F1 amplitude of 4 spikes/s as contrast threshold, I found that both TPMPA and JNJ16259685 significantly decreased ($p<0.01$) contrast thresholds of the RGCs.
Conclusions: Blocking either GABA-C or mGlu1 receptors improves the contrast response functions of RGCs in an animal model of retinitis pigmentosa.

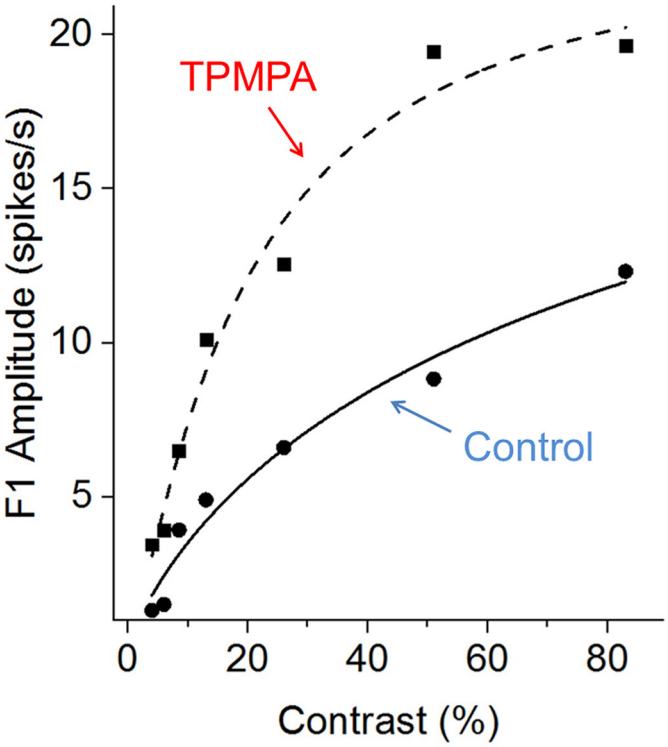

Effect of TPMPA on contrast response function of a P23H rat RGC
Commercial Relationships: Ralph J. Jensen, None
Support: Veterans Affairs RR&D Merit Review Award I01RX001299

Program Number: 2585 **Poster Board Number:** A0175
Presentation Time: 8:30 AM–10:15 AM
Distinct retinal ganglion cell subtypes exhibit diverse topographic characteristics across the mouse retina
Rana El-Danaf[1], Andrew Huberman[1, 2]. [1]Neurobiology, Stanford University School of Medicine, Stanford, CA; [2]Ophthalmology, Stanford Neurosciences Institute, BioX, Stanford University School of Medicine, Stanford, CA.
Purpose: As the sole output neurons of the retina, retinal ganglion cells (RGCs) possess an essential role for visual signal processing. Their loss is detrimental, as in neurodegenerative disorders like glaucoma- a leading cause of blindness. In recent years, the mouse has emerged as a premiere model for probing visual system disease, structure, and function. The general belief is that mice possess a relatively even topographic distribution of RGCs contrary to other species. Knowing that in mouse there are ~30 subtypes of RGCs each responding best to a specific feature in the visual scene, do different RGC subtypes possess topographic variations across the retina?
Methods: Different transgenic mouse lines were used to target five genetically-tagged RGC subtypes. These include: transient Off-alpha (tOff-α) RGCs labeled in the CB2-GFP transgenic mouse line (Huberman et al., 2008); posterior tuned On-Off direction selective RGCs (pOn-Off DSGCs) labeled in the TRHR-GFP transgenic mouse line (Rivlin-Etzion et al., 2011); Non-image forming "On" (NIF-On) and Non-image forming "diving" (NIF-diving) RGCs labeled in the Cdh3-GFP transgenic mouse line (Osterhout et al., 2011); and the W3-RGCs labeled in the TYW3 transgenic mouse line (Kim et al., 2010; Zhang et al., 2012). Using sharp electrodes, we injected fluorescent dyes intracellularly to fill individual RGCs at specific locations from across the retinal surface. We then evaluated their soma size and dendritic arbor extent according to their specific location using FIJI software.
Results: A total of 418 intracellularly labeled RGCs were analyzed. We discovered that 3/5 RGC subtypes exhibited dramatic topographic variations in arbor size. Each pattern of variation was distinct according to RGC subtype: pOn-Off RGCs displayed smaller dendritic fields in the ventral retina ($r^2 = 0.5648$), while smaller NIF-On RGCs were present in the nasal retina ($r^2 = 0.5822$) and W3-RGCs showed eccentricity related changes ($r^2 = 0.5356$).
Conclusions: Our results provide increasing evidence of the presence of topographic variations of RGC subtypes in the mouse retina; and that visual space is encoded in a region-specific manner such that certain visual features are sampled far more densely at some locations than others. A clearer understanding of how these different RGC subtypes are organized leads to insights into their role in visual processing, behavior and disease.
Commercial Relationships: Rana El-Danaf; **Andrew Huberman**, None
Support: NIH U01NS090562; The Glaucoma Research Foundation Catalyst for a Cure Initiative II

Program Number: 2586 **Poster Board Number:** A0176
Presentation Time: 8:30 AM–10:15 AM
Advanced Neural Circuit Analysis by Combining High-Resolution Optogenetic Stimulation, Two-Photon Imaging and Electrophysiology
Elric Esposito[1], Giulia Spampinato[2], Pierre Yger[3], Deniz Dalkara[4], Emiliano Ronzitti[5], Eirini Papagiakoumou[5], Valentina Emiliani[5], Serge A. Picaud[2], Olivier Marre[2], Jens Duebel[1]. [1]Neurophysiology and optogenetic applications in the retina, Sorbonne Universités, UPMC Univ Paris 06, INSERM, CNRS, Institut de la Vision, Paris, France; [2]Retinal information processing - Pharmacology and Pathology, Sorbonne Universités, UPMC Univ Paris 06, INSERM, CNRS, Institut de la Vision, Paris, France; [3]Computational neuroscience of sensory systems, Sorbonne Universités, UPMC Univ Paris 06, INSERM, CNRS, Institut de la Vision, Paris, France; [4]Gene therapies and animal models for neurodegenerative diseases, Sorbonne Universités, UPMC Univ Paris 06, INSERM, CNRS, Institut de la Vision, Paris, France; [5]Neurophotonics laboratory, Universtié Paris Descartes CNRS UMR8250, Paris, France.
Purpose: Investigation of retinal network activity of various retinal cells types remains a challenge, given current tools available. We developed a versatile optical instrument that allows for patterned single-photon (1P) / two-photon (2P) stimulation and simultaneous monitoring of neural activity through 2P imaging and electrophysiological recording.
Methods: We combined a two-photon (2P) laser scanning imaging system with a two-photon stimulation scheme using Spatial Light Modulator (SLM) based digital holography. The vast tuning range of the first laser output (680-1300nm) allows 2P imaging of a wide range of fluorophores, where the second output (fixed 1040 nm) is used for 2P stimulation of specific cells, transfected with optogenetic tools. The system further benefits from a digital micromirror device (DMD) projecting complex light pattern through the same high numerical aperture (NA = 1) objective. For electrophysiology, the setup is equipped with a patch-clamp rig for single cell analysis and a multi-electrode array (MEA) for population spike recording.
Results: The system provided high resolution 2P imaging (~0.5 mm XY, <2 mm Z) and 2P stimulation with an axial confinement under 50 µm for a 10 µm diameter spot. The setup was characterized through the MEA by patch-clamp recording of Human Embryonic Kidney (HEK) cells, transfected with a red-shifted microbial opsin (ReaChR) and stimulated at 1040 nm. The system was also used to stimulate

retinal interneuron cell activity while recording a large population of RGC's using the MEA.
Conclusions: We have designed a custom made optical system that not only can observe several retinal layers at high resolution, but can also control the activity of cells of interest, while recording electrical activity of post-synaptic cells. Combined with various optogenetic tools that can be expressed in specific cell types, our method will help to investigate the functional connections of neural microcircuits.
Commercial Relationships: Elric Esposito; **Giulia Spampinato**, None; **Pierre Yger**, None; **Deniz Dalkara**, None; **Emiliano Ronzitti**, None; **Eirini Papagiakoumou**, None; **Valentina Emiliani**, None; **Serge A. Picaud**, None; **Olivier Marre**, None; **Jens Duebel**, None
Support: ERC Optogenret 309776, NIH Grant U01NS09501

Program Number: 2587 **Poster Board Number:** A0177
Presentation Time: 8:30 AM–10:15 AM
Macular Ganglion Cell-Inner Plexiform Layer and Ganglion Cell Complex Thickness in 3000 Normal Chinese Children Aged 6-18 Years Old Using Swept-Source Opitcal Coherence Tomography
Mingjin Wang, Lu Cheng, Xiangui He, Minzhi Lv, Junjie Deng, Jianfeng Zhu, Haidong Zou, Xun Xu. Shanghai Eye Disease Prevention and Treatment Center, Shanghai, China.
Purpose: To investigate the normative value and distribution of macular ganglion cell-inner plexiform layer (GCIPL) and ganglion cell complex (GCC) thicknesses in normal Chinese school-aged children by swept-source longer-wavelength optical coherence tomography (SS-OCT), and to explore the associated factors with GCIPL and GCC thicknesses.
Methods: This was an observational cross-sectional study recruiting 3000 normal Chinese children aged 6 to 18 years old. Systemic parameters including age, gender, weight, height, and body mass index (BMI) were recorded. Comprehensive ophthalmic examinations, including axial length (AL), refractive error, intraocular pressure (IOP) and SS-OCT measurements were performed. Main outcome measures included macular GCIPL and GCC thicknesses, and their topographic variation in foveal (1-mm diameter area), parafoveal (1- to 3-mm diameter area), and perifoveal (3- to 6-mm diameter area) in the superior, temporal, inferior, and nasal field; minimum, maximum, 5%-95% interval, mean and standard deviation were recorded. The correlations between GCIPL/GCC thicknesses and age, gender, BMI, AL, refractive error, and IOP were analyzed as well. Right eyes of all subjects were selected for analysis.
Results: The mean age of the Children was 11.67 ± 3.44 years (male=1553, female=1447). The average thickness of GCIPL was 77.00±4.78 um (range: 42.33-97.44 um; 5%-95% interval: 69.56-84.56 um) and that of GCC was 107.68±5.95 um (range: 64-129.89 um; 5%-95% interval: 98.45-117.21 um). A thicker GCIPL was associated with male gender (standard coefficient=0.168, $p<0.001$), older age (standard coefficient=0.126, $p<0.001$), AL (standard coefficient=-0.181, $p<0.001$) and refraction error (standard coefficient=0.233, $p<0.001$), but not with BMI or IOP in the multiple regression model ($R^2=0.13$). Meanwhile, age (standard coefficient=0.154, $p<0.001$), gender (standard coefficient=0.102, $p<0.001$) and refraction error (standard coefficient=0.149, $p<0.001$) were associated independently with GCC thickness ($R^2=0.12$) after adjusted for other systematic and ocular factors.
Conclusions: Using SS-OCT, normative macular GCIPL and GCC thicknesses in healthy children below 18 years were established. Age, gender, and refraction error were related to both GCIPL and GCC thicknesses.
Commercial Relationships: Mingjin Wang, None; **Lu Cheng**, None; **Xiangui He**, None; **Minzhi Lv**, None; **Junjie Deng**, None; **Jianfeng Zhu**, None; **Haidong Zou**, None; **Xun Xu**, None

Program Number: 2588 **Poster Board Number:** A0178
Presentation Time: 8:30 AM–10:15 AM
Genetic dissection of photoreceptor contributions to the mouse ganglion cell receptive field
Robert L. Seilheimer[1, 2], Jasdeep Sabharwal[1, 2], Samuel M. Wu[1]. [1]Ophthalmology, Baylor College of Medicine, Houston, TX; [2]Medical Scientist Training Program, Baylor College of Medicine, Houston, TX.
Purpose: The retinal ganglion cell (RGC) receptive field represents the cell's space-time processing. While the connectivity of cells in the retina is well characterized, the functional implications of this circuitry on the RGC receptive field are poorly understood. In this study, we use white noise stimulation and multi-electrode recording to map RGC receptive fields in rod and cone knockout (Trα -/- and GNAT2 -/-) mice to characterize the effect of removing rods on the spatiotemporal processing of RGCs.
Methods: Retinas from 12-16 week old dark-adapted male mice (3 C57/B6 and 1 Trα -/-) were whole-mounted on a multi-electrode array for extracellular recording of ganglion cell action potentials. Retinas were stimulated with binary white noise checkerboards at 15 Hz at both scotopic and photopic light levels. Single units (70 C57/B6 and 12 Trα -/-) were isolated from recordings and spike-triggered averages (STAs) were computed for each unit to map ganglion cell space-time receptive fields. STAs were fit with a spatiotemporal model composed of a difference of Gaussians spatial model and the impulse response function of a bandpass filter. Parameters of these models were used to compare RGC properties.
Results: Our results show differences in spatiotemporal processing between wild type and Trα -/- mice. First, RGCs in the Trα -/- mouse had responsive STAs under photopic but lacked them under scotopic conditions, while those in wild-type mice had responsive STAs in both conditions. Comparing the photopic receptive fields, the Trα -/- RGCs had faster temporal processing in their center than wild type cells. However, we see that knockout of Trα -/- has no effect on the antagonistic surround, as it is present in both groups of RGCs. Lastly, we saw no change in RGC receptive field center size in the Trα -/- mouse.
Conclusions: By combining white noise analysis with genetic knockout of rods and cones, we can single out their contribution to the receptive field of retinal ganglion cells. Unsurprisingly, rods are necessary for RGC spatiotemporal processing in dim light. Further, consistent with their longer integration time, we find that RGC temporal processing is faster in the absence of rods. Lastly, we see that rods have no effect on gross spatial processing in RGCs in photopic conditions. Investigation of spatiotemporal properties of RGCs in mice without cones is underway.
Commercial Relationships: Robert L. Seilheimer, None; **Jasdeep Sabharwal**, None; **Samuel M. Wu**, None
Support: NIH grants EY004446, EY019908, EY002520, and EY007001, the Retina Research Foundation (Houston), Research to Prevent Blindness, Inc., and the BRASS Foundation

Program Number: 2589 **Poster Board Number:** A0179
Presentation Time: 8:30 AM–10:15 AM
Retinal Ganglion Cells Layer thickness as a possible bio-marker for accelerate ageing due to Human Immunodeficiency Virus infection
Alessandro Invernizzi[1, 2], Alessandra Acquistapace[1], Sara Bochicchio[1], Chiara Resnati[3], Simone Pomati[4], Alexander Klistorner[2], Giovanni Staurenghi[1], Agostino Riva[3].
[1]Department of Biomedical and Clinical Science "Luigi Sacco", University of Milan, Milan, Italy; [2]Save Sight Institute - University of Sydney, Sydney, NSW, Australia; [3]Department of Clinical Sciences, Luigi Sacco Hospital, Section of Infectious and Tropical Diseases, University of Milan, Milan, Italy; [4]Center for Research and Treatment on Cognitive Dysfunctions, Institute of Clinical Neurology, Department of Clinical Sciences, Luigi Sacco Hospital, University of Milan, Milan, Italy.
Purpose: To measure the thickness of different retinal layers by spectral domain optical coherence tomography (SD-OCT) in patients affected by Human Immunodeficiency Virus (HIV) with well controlled disease, and to correlate it with subject age, sex, disease duration, CD4 nadir, use of thymidine analogues, and cognitive status.
Methods: HIV subjects with well controlled disease between 40 and 70 years, and sex- age-matched controls were enrolled. On one eye from each subject Ganglion cells layer (GCL), Inner Plexyform Layer (IPL) and Outer Nuclear Layer (ONL) thickness was assessed on a 30x25 degrees SD-OCT volume centered onto the fovea by an automatic segmentation algorithm (Eye Explorer 1.9.10.0, Heidelberg). Mean thickness was calculated for each layer. Retinal Nerve Fiber Layer (RNFL) thickness was automatically calculated on a circumpapillary scan. Layers' thickness was compared between HIV patients and controls. The effect of age and sex on the thickness of all the studied layers was tested through a multivariate regression analysis in both groups. In HIV patients the same analysis also considered disease duration, CD4+ nadir, use of thymidine analogues, and cognitive status of the patient (assessed through Montreal Cognitive Assessment (MoCA)Test).
Results: Sixtynine HIV patients (21 females; age 53±7,3 years) and 65 age- and sex- matched controls were enrolled. No significant difference in the thickness of any of the studied layers was found between the two groups. In HIV subjects thickness of GCL and IPL significantly decreased with age (p=0.001 and p=0.02 respectively). This was not seen in controls. ONL and RNFL didn't show changes with ageing. Gender didn't affect any of the layers' thickness in both groups. MoCA Test score significantly decreased with ageing much more in HIV subjects (p=0.0009) than in controls (p=0.047). In the HIV group a positive correlation was found between GCL thickness and MoCA Test score (p=0.04). In HIV patients, layers' thickness was not influenced by disease duration, CD4+ nadir and use of thymidine analogues.
Conclusions: GCL and IPL thickness is strongly correlated with age in HIV subjects. This doesn't happen in controls. GCL thickness and cognitive function are correlated in HIV subjects. GCL thickness could be a possible biomarker for central nervous system accelerate ageing induced by chronic HIV infection.
Commercial Relationships: Alessandro Invernizzi; **Alessandra Acquistapace**, None; **Sara Bochicchio**, None; **Chiara Resnati**, None; **Simone Pomati**, None; **Alexander Klistorner**, None; **Giovanni Staurenghi**, Pfizer (C), Ocular Instruments (P), Optos (C), OD-OS (C), Zeiss (S), GlaxoSmithKline (C), Bayer (C), QLT Phototherapeutics (C), Optovue (S), Heidelberg Engineering (C), Canon (C), Alcon (C), Allergan (C); **Agostino Riva**, None

Program Number: 2590 **Poster Board Number:** A0180
Presentation Time: 8:30 AM–10:15 AM
Study of Regulatory Mechanism of Growth Differentiation Factors on Retinal Ganglion Cell Development
Kun-Che Chang, Catalina Sun, Xin Xia, Suqian Wu, Jeffrey L. Goldberg. Ophthalmology, Stanford University, Palo Alto, CA.
Purpose: What regulates neuronal differentiation and integration into mature circuits in the retinal ganglion cell (RGC)? This question has begun to be studied in neural development but also strongly impacts the adult nervous system. Growth and differentiation factor-11 (GDF-11) has been reported in neurogenesis. Here we evaluated the influence of GDF-11 and -15 on RGC fate specification.
Methods: Embryonic day 14 (E14), postnatal day 0 (P0), postnatal day 2 (P2) retinas were dissected from wild type (WT), Chx10-Cre/GDF-11 cKO and GDF-15 KO mice ($N \geq 6$), respectively. Expression levels of marker genes and proteins with and without GDF treatment were determined by QPCR, Western blot and immunofluorescence staining. This research was conducted in compliance with the ARVO Statement for the Use of Animals in Ophthalmic and Vision Research. Data were analyzed by ANOVA with Tukey's test with *P* value of <0.05 considered statistically significant.
Results: As measured by QPCR, RGC marker gene Brn3a was significantly upregulated in P0 GDF-11 KO retinas (p=0.016). Less Brn3a staining was observed in P2 GDF-15 KO retinas. Five days of GDF-11 treatment of E14 retinas downregulated the expression of RGC transcriptional regulators Math5 and Neurog2 and RGC marker genes Brn3a and RBPMS (p<0.05). In addition, RGC fate suppressing factors Notch1 and Hes5 were induced by GDF-11 (p<0.05). Smad2 was activated by GDF-11 but not GDF-15. Pharmacologic blockade of Smad2 signaling rescues GDF-11-reduced RGC fate and marker genes expression (p<0.05). Interestingly, pretreatment with GDF-15 attenuated GDF-11-induced phospho-Smad2 activation.
Conclusions: In this study, we investigate the effect of GDF-11 and -15 in developmental retina and reveal the regulatory mechanism *in vivo* and *ex vivo*. GDF-11 plays a suppressive role in RGC fate specification by activating Smad2-mediated Notch signaling. GDF-15 neutralizes GDF-11-mediated Smad2 activation and suppression of RGC differentiation, thereby promoting RGC fate specification. Understanding the role of GDFs in retina may provide a therapeutic strategy for RGC differentiation when considering cell replacement therapies.

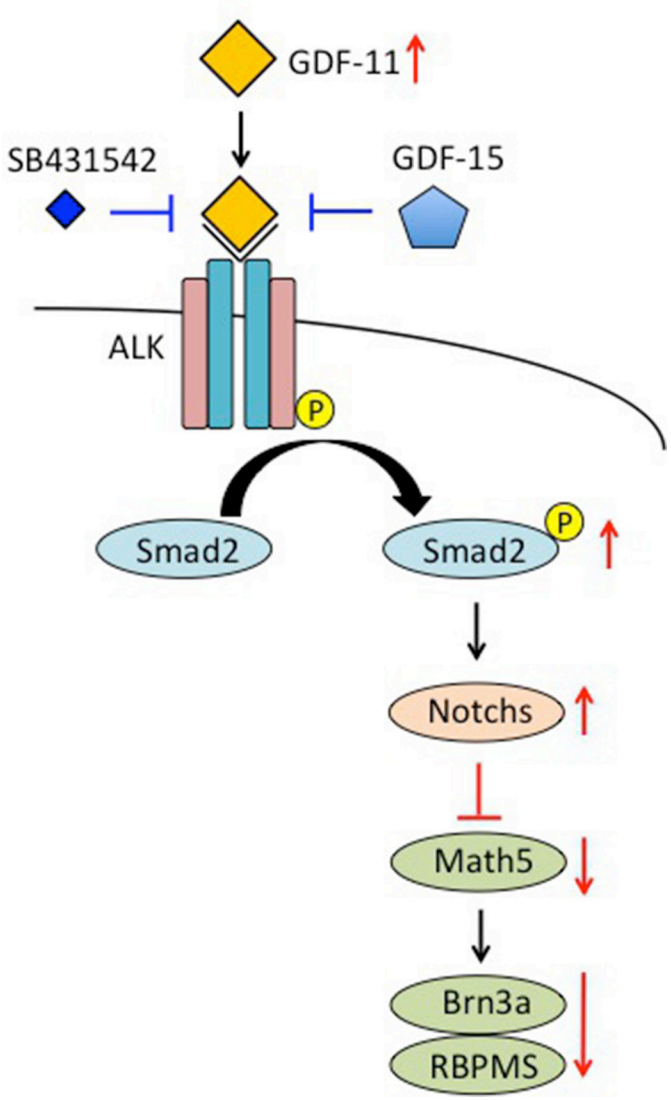

Mechanism of GDF-11 on RGC fate specification

Commercial Relationships: Kun-Che Chang, None; **Catalina Sun**, None; **Xin Xia**, None; **Suqian Wu**, None; **Jeffrey L. Goldberg**, None

Program Number: 2591 **Poster Board Number:** A0181
Presentation Time: 8:30 AM–10:15 AM

Retinoid-related orphan receptorβ regulates the balance of ipsilateral and contralateral ganglion cells in mouse retina

In-Jung Kim, Jonathan B. Demb, Haewon Byun. Ophthalmology, Yale School of Medicine, New Haven, CT.

Purpose: Retinal ganglion cells (RGCs) convey the retinal output to the brain and divide into two groups according to their axonal projections: ipsilaterally-projecting RGCs (ipsi-RGCs) project to the same hemisphere, whereas contralaterally-projecting RGCs (contra-RGCs) cross and project to the opposite hemisphere. The ratio of ipsi-RGCs to contra-RGCs determines the extent of binocular vision, which supports depth perception. Here, we investigated a novel mechanism, mediated by retinoid-related orphan nuclear receptor β (Rorβ), that regulates the balance between ipsi- and contra-RGCs.
Methods: Using a gain-of-function approach, we delivered Rorβ DNA into the eyes of the embryonic day 13 (E13) control mouse, via *in utero* electroporation, and examined retinas at E16 or E18. Using a loss-of-function approach, we studied the Rorβ knock-in mouse, in which the open reading frame of green fluorescent protein replaces the Rorβ1 specific exon (Liu et al., 2013: kindly provided by D. Forrest at NIDDKD). Retinas from control and mutant mice were analyzed at E11-E18. Ipsi-RGCs were visualized with an antibody to Zic2, and contra-RGCs were visualized with antibodies to Brn3a and Isl2. Labeled cells were visualized with confocal microscopy and quantified across 6-9 sections from 3-4 animals.
Results: Overexpression of Rorβ in embryonic retina led to the overproduction of contra-RGCs and underproduction of ipsi-RGCs. Deletion of Rorβ led to the opposite phenotype: delayed differentiation of contra-RGCs and overproduction of ipsi-RGCs. In addition, deletion of Rorβ decreased the level of sonic hedgehog (Shh), which is normally expressed exclusively in contra-RGCs and negatively regulates development of ipsi-RGCs (Sánchez-Arrones et al., 2013). These data suggest that Shh could act as a downstream mediator of Rorβ.
Conclusions: Rorβ regulates the propagation of contra-RGC differentiation and is both necessary and sufficient for generating the balance of ipsi-RGCs to contra-RGCs. Our data show for the first time that disrupting the timing of contra-RGC development alters the relative specification of ipsi- and contra-RGCs. These results reveal a novel molecular mechanism for regulating the ratio of ipsi- to contra-RGCs and thereby establishing healthy binocular vision.
Commercial Relationships: In-Jung Kim, None; **Jonathan B. Demb**, None; **Haewon Byun**, None
Support: R00 EY019355, the Whitehall Foundation, the E. Matilda Ziegler Foundation and an unrestricted grant from Research to Prevent Blindness to Yale University.

Program Number: 2592 **Poster Board Number:** A0182
Presentation Time: 8:30 AM–10:15 AM

Promoting optic nerve regeneration with a novel biocompatible fibrous scaffold

Karen Chang[1, 2], Jhih-Guang Wu[3], Kin-Sang Cho[2], Shyh-Chyang Luo[3], Ta-Ching Chen[4], Min-Huey Chen[1], Wei-Fang Su[3], Dong F. Chen[2]. [1]Graduate Institute of Clinical Dentistry, School of Dentistry, National Taiwan University, Taipei, Taiwan; [2]Department of Ophthalmology, Schepens Eye Research Institute and Massachusetts Eye and Ear, Boston, MA; [3]Department of Materials Science and Engineering, National Taiwan University, Taipei, Taiwan; [4]Department of Ophthalmology, National Taiwan University Hospital, Taipei, Taiwan.

Purpose: Glaucoma, a neurodegenerative disease, leads to progressive nerve damage and eventually loss of vision. Once the degeneration is occurred, it is permanent and irreversible. The purpose of this study is to develop a biocompatible scaffold for promoting retinal ganglion cells (RGC) survival and optic nerve regeneration after injury.
Methods: Polycaprolactone (PCL) and poly-gamma-benzyl-L-glutamate (PBG) fibrous scaffolds were prepared by 3D electrospinning with different fiber arrangements. To investigate the biocompatibility of those scaffolds, retinal ganglion cell progenitors (RGCP) were cultured on either aligned fibers or non-aligned fibers of PBG or PCL scaffolds for 1, 5, 10 days respectively. Cell survival, morphology, as well as neurite outgrowth rate and neurite length were observed by immunocytochemistry staining characterization.
Results: The biomimetic electrospun scaffolds for PCL and PBG featuring uniform fibrous structures and three dimensional porous networks. PBG scaffold with aligned fibers were successfully fabricated, supporting cell survival and robust growth of long neurite along the direction of the fibers.

Conclusions: The aligned PBG scaffold showed a great potential to assist RGCP differentiation and growth. Such scaffold may not only be beneficial for optic nerve regeneration, but also have a wide range of applications for tissue engineering on future regenerative medicine.
Commercial Relationships: Karen Chang; **Jhih-Guang Wu**, None; **Kin-Sang Cho**, None; **Shyh-Chyang Luo**, None; **Ta-Ching Chen**, None; **Min-Huey Chen**, None; **Wei-Fang Su**, None; **Dong F. Chen**, None
Support: MOST (105-2917-I-002-031), NIH/NEI (R41 EY025913 and R01EY025259), the Core Grant for Vision Research from NIH/NEI to the Schepens Eye Research Institute (P30EY03790)

Program Number: 2593 **Poster Board Number:** A0183
Presentation Time: 8:30 AM–10:15 AM
Regulation of neurite growth by IGFBP family members
Yingqian Li, Kin-Sang Cho, Dong F. Chen. Chen lab, Schepens Eye research institute, Boston, MA.
Purpose: Activation of axonal growth program is a critical step in successful nerve regeneration following injury. As a standard model of CNS neurons, retinal ganglion cells (RGCs) shut down the intrinsic axon growth program during the perinatal period in mice. We found previously that insulin-like growth factor binding protein like protein-1 (IGFBPL1) functions as a secretory factor that positively regulates RGC axonal outgrowth *in vitro* through mediating IGF-1 signaling pathways. This prompts us to examine the roles of other IGFBPs in IGF-1-mediated neurite growth in neurons, particularly RGCs.
Methods: The expression levels of IGFBP family members were quantatively assessed in purified RGCs of wild type and *Igfbpl1* deficient mice at different ages: embryonic day 16 (E16), postnatal day 0 (P0) and P10 by q-PCR. These ages are before and after RGCs lose their ability to regenerate axons. In addition, we studied the capacity of these binding proteins in mediating neurite outgrowth in NGF-induced PC12 cell cultures. Percentage of cell bearing neurite, cell survival rate and average neurite length were quantified under a masked fashion.
Results: We found that the levels of IGFBP7 changed drastically before and after RGCs lose their ability to regenerate axons. Interestingly, the expression levels of many IGFBP family members showed dramatic changes in *Igfbpl1* KO mice when compared with wild type mice, including IGFBP7. Addition of IGFBP7 to PC12 cell cultures inhibited neurite outgrowth in a dose-dependent manner, without affecting cell survival.
Conclusions: Our results suggest that IGFBP family members are important players, acting as either a negative or positive regulator, in mediating RGC neurite outgrowth.
Commercial Relationships: Yingqian Li, None; **Kin-Sang Cho**, None; **Dong F. Chen**, None
Support: NIH/NEI (R41 EY025913 and R01EY025259), the Core Grant for Vision Research from NIH/NEI to the Schepens Eye Research Institute (P30EY03790)

Program Number: 2594 **Poster Board Number:** A0184
Presentation Time: 8:30 AM–10:15 AM
Development of Intrathalamic Connections Between dLGN and TRN
Peter W. Campbell, William Guido. Anatomical Sciences & Neurobiology, University of Louisville, Louisville, KY.
Purpose: The reciprocal connections between the dorsal lateral geniculate nucleus (dLGN) and the thalamic reticular nucleus (TRN) play an important role in regulating thalamocortical activity during different behavioral states such as attention, wakefulness, and sleep. Axon collaterals of thalamocortical neurons provide feedforward excitatory input onto GABAergic TRN neurons, which in turn convey feedback inhibition to dLGN relay neurons. Here we examined when and how these circuits arise during early postnatal life.
Methods: We employed mouse transgenics to visualize when inputs appear and optogenetics to assess when functional patterns of connectivity emerge. To determine when projections arrived in their target nucleus, we examined coronal sections across multiple early-postnatal ages using confocal microscopy. We also studied when these connections became functional by combining optogenetics with *in vitro* whole cell patch clamp physiology.
Results: Our results show that TRN terminals arrive in dLGN at early postnatal ages and span the entire nucleus in a diffuse but dense plexus by the end of the first postnatal week. Weak inhibitory postsynaptic activity from TRN to dLGN appears during the first postnatal week, and grows steadily in amplitude to reach adult-like levels by the third postnatal week. Feedforward excitatory connections from dLGN to TRN begin to arrive near the end of the first postnatal week. Soon after, weak excitatory responses appear and mature rapidly, reaching adult-like levels by the third postnatal week.
Conclusions: Taken together, these data suggest that reciprocal connections between dLGN and TRN develop in a coordinated manner, with feedback inputs arising somewhat earlier that feedforward ones. The emergence of this intrathalamic loop occurs well after retino-geniculate and geniculo-cortical connections are established and at about the same time as descending corticothalamic connections are made with TRN and dLGN. Thus it would appear that circuits involved in the state dependent modulation of sensory signal transmission are assembled after primary visual pathways are established.
Commercial Relationships: Peter W. Campbell, None; **William Guido**, None
Support: NEI Grant EY012716-17

Program Number: 2595 **Poster Board Number:** A0185
Presentation Time: 8:30 AM–10:15 AM
Pou4f1/Brn3a regulates neurite- and synapse-associated genes during Retinal Ganglion Cell development
Vladimir Muzyka, Tudor C. Badea. National Eye Institute, NIH, Bethesda, MD.
Purpose: The Pou4f/Brn3 family of POU-domain transcription factors regulates the development of the majority of retinal ganglion cells (RGCs). Brn3a, one of the three family members, is expressed in a subset of RGCs, and is required for the development of specific RGC types, with dense, small area dendritic arbors. Loss of Brn3a also affects the morphology of other RGC subtypes. Currently, it is not clear what molecular mechanisms and genes are responsible for the specification of those cells during development, and how Brn3a regulates it.
Methods: Our group has previously performed a large-scale RNA sequencing screen for molecules (Sajgo, Ghinia and Badea, unpublished) regulated by Brn3-s in RGCs at postnatal day 3. We now use RT-PCR, *in situ* hybridization and protein immuno-detection in $Brn3a^{KO}$ retinas and controls in order to validate several of the potential targets and describe their expression profile during postnatal RGC development.
Results: We describe the expression profiles of 28 potential Brn3a-RGC target genes at several postnatal ages, beginning with P0 (postnatal day 0) and into the adult age. The genes comprise transcription factors, posttranscriptional regulators, enzymes, trafficking, signaling and adhesion molecules. We find that, whereas most of the identified targets exhibit RGC specificity and/or Brn3a dependency at the screening target age (P3), many of them change

their expression profile dynamically, and only a fraction preserve RGC specificity throughout postnatal development into adulthood.
Conclusions: The Pou4f1/Brn3a dependent RGC transcriptional program consists of at least 20 genes and/or transcripts. Some of these are RGC specific, while others are dynamically expressed in RGCs and/or other retinal cell types at different developmental stages. Based on conserved domain structure and previously published evidence many of the identified molecules could be involved in dendrite morphology formation and synaptogenesis.
Commercial Relationships: Vladimir Muzyka, None; **Tudor C. Badea**, None

Program Number: 2596 **Poster Board Number:** A0186
Presentation Time: 8:30 AM–10:15 AM
Dendritic reorganization of starburst amacrine cells secondary to retinal ganglion cell death
Ning Tian[1], Tao He[2, 1], Xavier Mortensen[1], Ping Wang[1]. [1]Ophthalmology & Visual Science, University of Utah, Salt Lake City, UT; [2]Ophthalmology, Wuhan University, Wuhan, China.
Purpose: To quantify surviving and dendritic reorganization of starburst amacrine cells secondary to retinal ganglion cell (RGC) death due to optic nerve crush (ONC) and the possible role of CD3ζ mediated signals in the dendritic development and degeneration of starburst amacrine cells.
Methods: ONC was performed unilaterally in mice expressing YFP in starburst amacrine cells with or without mutation of a key component of T-cell receptor complex, CD3ζ. Cells in the ganglion cell layer (GCL) labeled by DAPI, ChAT-positive cells in both GCL (displaced starburst amacrine cell, DSAC) and inner nuclear layers (INL, conventionally located starburst amacrine cell, SAC) were quantified for cell density 7 or 10 days after ONC. Individual YFP-expressing starburst amacrine cells were imaged using confocal microscopy and their dendrites were quantified using Neurolucida software.
Results: Dendritic architectures of SACs and DSACs are significantly different. The ONC procedure caused 31% cell loss in the GCL 10 days after ONC. However, SACs and DSACs lose their dendrites by 24% and 20% respectively without cell death. In CD3ζ mutants, the size of dendritic field of DSACs was increased by 38%, the dendritic length of SACs were decreased by 10% and the cell density was increased by 19%. However, mutation of CD3ζ has no significant effect on RGC death or dendritic reorganization of starburst amacrine cells after ONC.
Conclusions: RGC death caused by ONC is associated with immediate dendritic reorganization of starburst amacrine cells. CD3ζ regulates the development of dendritic architecture of starburst amacrine cells but not dendritic reorganization of these cells after RGC death.
Commercial Relationships: Ning Tian, None; **Tao He**, None; **Xavier Mortensen**, None; **Ping Wang**, None
Support: NIH grants R01 EY012345 and P30 EY014800, VA grant 1 I01 BX002412, Research to Prevent Blindness (RPB), Funds from the John Moran Eye Center, China Scholarship Council (CSC) 201406275047.

Program Number: 2597 **Poster Board Number:** A0187
Presentation Time: 8:30 AM–10:15 AM
Differential expression and distribution of Copines in Retinal Ganglion Cells
Manvi Goel, Tiansen Li, Tudor C. Badea. National Eye Institute, National Institutes of Health, Bethesda, MD.
Purpose: The role of Brn3 transcription factors in development of cell-specific dendritic arbors and synapse formation in the inner retina is not clearly understood. Brn3s regulate several genes in the retina that might have an important role in synapse formation. From the RNA sequencing done previously in our lab on wild –type and Brn3b $^{-/-}$ mouse retinas and purified RGCs, we identified a family of proteins-Copines which are regulated by Brn3b. Copines are intracellular proteins containing two C2 domains and an integrin like von Willebrand A domain. In this work, we investigate the distribution pattern of different Copines in the retina.
Methods: There are nine Copines (1 to 9) present in the mammalian genome. Based on RNAseq data we predicted that 5 of them are differentially expressed in RGCs. We studied their expression in the inner retina, specifically in the RGCs, using in-situ hybridization. Cell type specific expression pattern was studied using immunohistochemistry (IHC) with commercially available and in-house antibodies for different Copines. The sub-cellular distribution of some of these Copine family members was also studied using IHC in a Cre dependent expression in Brn3b RGCs after intraocular injection with AAV constructs for the Copines.
Results: Five Copine proteins are differentially expressed in the retina starting from early postnatal ages and have a dynamic expression through the retinal development. The different copines have a differential expression pattern in the RGCs and amacrine cells. The sub-cellular localization for the Copines indicate their presence in cell bodies as well as the dendrites of the RGCs.
Conclusions: Our results show the differential expression of several Copines in the inner retina and also their sub-cellular localization within the Brn3b positive RGCs. Owing to the differences in their expression pattern and sub-cellular localization, the different Copines might participate in a combinatorial, cell type specific fashion in dendrite development and synaptogenesis in the inner retina.
Commercial Relationships: Manvi Goel, None; **Tiansen Li**, None; **Tudor C. Badea**, None

Program Number: 2598 **Poster Board Number:** A0188
Presentation Time: 8:30 AM–10:15 AM
The Orientation of Mouse Retina from Ocular Landmarks: Where you cut matters
Katelyn Sondereker[1], Sean Hahghgou[2], Jessica Onyak[1], Jordan M. Renna[1], Maureen Stabio[2]. [1]Department of Biology, The University of Akron, Akron, OH; [2]Department of Cell and Developmental Biology, University of Colorado School of Medicine, Denver, CO.
Purpose: The anatomical orientation of the retina with respect to the mouse orbit is relevant for research studies of opsin distribution, retinal degeneration, direction selective retinal ganglion cells, melanopsin ganglion cells, and retinal cell taxonomy. In particular, many studies have found that functionally distinct retinal ganglion cells have density and size gradients across the mouse retina. However, a review of the literature indicates that different groups report different methods to mark the topographic orientation of the retina (dorsal, ventral, temporal and nasal poles). Such variations in retinal landmark identification may result in discrepancies in the topographic distribution of retinal cells (such as melanopsin ganglion cells) as reported by different studies. The goal of this project was to create an accurate anatomical map of the mouse retina that includes all commonly used landmarks, including the rectus muscles, choroid fissure, temporal canthus, dorsal corneal, and opsin gradient.
Methods: Four methods were followed as described in the literature to identify physical landmarks during enucleation and retinal isolation in adult C57 mice: 1) dorsal corneal burn, 2) tattoo dye at the temporal canthus, 3) cuts at rectus muscle insertion points, and 4) cuts at the temporal-nasal points of the choroid fissure. Retinas were fixed in 4% PFA, stained with s-opsin, imaged with Leica-TCS-SP5

confocal microscope, and analyzed with Leica-LASAF and ImageJ. All retinas were digitally re-stitched with Retistruct and aligned to the s-opsin gradient; polar plots of retinal landmarks were compared in Origin.
Results: The rectus muscles were measured at 19.2±6.3, 82.0±9.6, 169.3±14.7, and 259.4±15.8 degrees for medial, superior, lateral, and inferior rectus, respectively (n=8). Nasal and temporal choroid fissure landmarks were measured at 7.5±3.1 and 172.3±8.5 degrees, respectively (n=8), and temporal and dorsal landmarks at 187.5±13.2 and 98.4±23.9 degrees, respectively (n=8). However, a 15 degree mismatch was found between choroid fissure and medial/lateral rectus landmarks. The lowest internal consistency was found in the dorsal burn dissection method.
Conclusions: These results suggest that variations in dissection methods and retinal cuts may be a source of discrepancy between studies that use different dissection techniques to orient the retina.
Commercial Relationships: Katelyn Sondereker, None; **Sean Hahghgou**, None; **Jessica Onyak**, None; **Jordan M. Renna**, None; **Maureen Stabio**, None

Program Number: 2599 **Poster Board Number:** A0189
Presentation Time: 8:30 AM–10:15 AM
Plastic changes in ganglion cell spectral responses after transgenic manipulation of the zebrafish cone mosaic
Leah J. Middleton, Ralph F. Nelson. National Institute of Neurological Disorders and Stroke, National Institutes of Health, Bethesda, MD.
Purpose: The tetrachromatic (red, green, blue and UV cone) zebrafish overproduces red cones at the expense of other types upon transgenic miss-expression of the thyroxin β2 nuclear receptor (trβ2) in all photoreceptor progenitors (Suzuki et al., 2013). We examine the impact of this perturbation on retinal circuits for wavelength discrimination seen in retinal ganglion cells (rGCs).
Methods: The spectral sensitivities of rGCs were recorded in both wildtype (WT) and crx:trβ2 larvae at 5, 6, 7, and 11 or 12 dpf. Eyes were removed, inverted to expose the optic nerve, stabilized with a droplet of agarose, and perfused with oxygenated MEM while a microelectrode (with 500μM NaCl) was inserted into the optic nerve to record single-fiber spike responses. Eyes were exposed to 280 spectral stimuli covering 9 wavelengths (330-650nm). Spectra were fit by a 'sum of Hill functions' model. Responses of 44 WT and 55 crx:trβ2 rGCs were categorized by temporal and spectral properties. The distribution of rGCs across these categories was compared between WT and crx:trβ2 fish using a chi-squared test.
Results: ON rGCs were less frequent ($p = 0.05$) in crx:trβ2 as compared to WT, but ON-OFF rGCs were more frequent ($p < 0.0001$). Light offset responses of crx:trβ2 ON-OFF and OFF cells more frequently responded to red cones ($p < 0.05$), but were less frequently responsive to green ($p < 0.05$), blue ($p < 0.05$), and UV ($p < 0.001$) inputs. A greater proportion of light offset components were driven solely by red cone inputs ($p < 0.05$). Interestingly, at light onset, the frequency of rGCs excited or inhibited by green ($p = 0.255$), blue ($p = 0.987$), or UV cones ($p = 0.228$) did not differ. In crx:trβ2 rGCs, a greater proportion of cells were inhibited at stimulus onset by red cones ($p < 0.001$), but a similar proportion were excited at light onset by red cones ($p = 0.082$).
Conclusions: Despite reduced density of green, blue, and UV cones in crx:trβ2, at light onset, rGCs were just as frequently excited or inhibited by these pathways, suggesting a circuitry compensation. The greater proportion of onset responses with red-cone inhibition suggests circuitry reorganization, as does the greater frequency of light offset responses to red cones, many of which are driven solely by red cones. The more robust OFF-pathway in crx:trβ2's results in a greater proportion of ON-OFF rGCs.
Commercial Relationships: Leah J. Middleton, None; **Ralph F. Nelson**, None

Program Number: 2600 **Poster Board Number:** A0190
Presentation Time: 8:30 AM–10:15 AM
MicroRNA-19a enhances axon regeneration in retinal ganglion cells
Heather K. Mak[1], Xu Cao[1], Jasmine S. Yung[1], Heidi Ng[1], Tin Lap Lee[2], Christopher K. Leung[1]. [1]Ophthalmology and Visual Sciences, The Chinese University of Hong Kong, Hong Kong, Hong Kong; [2]School of Biomedical Sciences, The Chinese University of Hong Kong, Hong Kong, Hong Kong.
Purpose: Retinal ganglion cells (RGCs) lose capacity to regenerate axons in early postnatal age. While a number of transcription factors and signaling molecules have been implicated to the loss of regenerative potential of RGC axon, their upstream regulators are largely unstudied. We investigated the association between developmental decline of RGC regenerative potential and age-related changes in microRNA (miRNA) expression and demonstrated that miRNA-19a augments RGC axon regenerative capacity after optic nerve (ON) injury.
Methods: Microarray was performed on purified RGCs from Sprague Dawley (SD) rats at embryonic day 21 (E21), postnatal day 6 (P6), postnatal day 14 (P14), and postnatal day 30 (P30) to study the changes in miRNA expression. Age-related change in miRNA expression was confirmed by RT-PCR. RGC axon length and growth rate from SD rats and human adult donor eyes were measured by microfluidic chambers (MFCs) and time-lapse imaging, respectively, after transduction of AAV-miR-19a-eGFP or control. C57BL/6 mice were intravitreally injected with AAV-miR-19a-eGFP or control 2 weeks before ON crush and the number of regenerating axons was measured 4 weeks after crush.
Results: Microarray revealed 65 miRNAs to be significantly downregulated from E21 to P30 in which RT-PCR confirmed that miR-19a decreased 55-fold from E21 to P30 ($p<0.001$). miR-19a increased RGC axon length in MFCs by 2.62- and 2.01-fold on 14 and 21 days *in vitro*, respectively ($p<0.006$), and accelerated axon regenerative growth rate by 2.46-fold ($p<0.001$) in time-lapse imaging compared with controls. Human adult RGCs with miR-19a had longer axon and total neurite lengths by 26.7% ($p=0.025$) and 59.8% ($p<0.001$), respectively, compared with controls. Mice with miR-19a had 2-folds more regenerated axons ($p=0.004$) at every 0.5 mm starting 1 mm from the ON crush site.
Conclusions: There is an age-related change of miRNA levels in RGCs, which coincides with the age-related decline in axon growth potential. We showed that the loss of axon regenerative potential can be partially restored by upregulating miR-19a in RGCs *in vitro* and *in vivo*, presenting a new potential therapeutic approach to resuscitate age-related loss of axon growth ability.

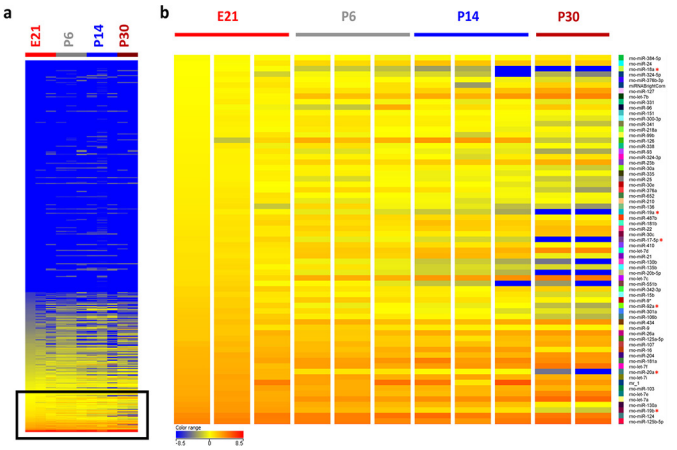

Heirarchical cluster of E21, P6, P14, and P30 RGC miRNA and 65 miRNAs significantly downregulated from E21 to P30.

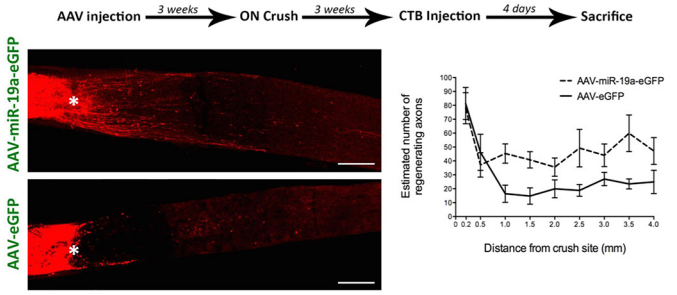

ON sections after crush with AAV-miR-19a-eGFP (*top*) or AAV-eGFP (*bottom*), and estimated number of regenerated axons.

Commercial Relationships: Heather K. Mak, None; **Xu Cao**, None; **Jasmine S. Yung**, None; **Heidi Ng**, None; **Tin Lap Lee**, None; **Christopher K. Leung**, Alcon (R), Santen (R), Merck (R), Oculus (F), Alcon (C), Carl Zeiss Meditec (F), Glaukos (F), Allergan (R), Carl Zeiss Meditec (P), Optovue (F), Global Vision (R), Tomey (F), Tomey (R), Novartis (R), Lumenis (R), Topcon (F), Allergan (C)